Available online at www.sciencedirect.com
ScienceDirect
Journal of Organometallic Chemistry 691 (2006) 4400–4410
Journal of Organometallic Chemistry
www.elsevier.com/locate/jorganchem

Hydrosilylation vs. [2 + 2]-cycloaddition: A theoretical study with iron and ruthenium complexes

Uwe Böhme *

Institut für Anorganische Chemie, TU Bergakademie Freiberg, Leipziger Str. 29, D 09596 Freiberg, Germany

Received 17 October 2005; received in revised form 5 January 2006; accepted 12 January 2006
Available online 21 February 2006

Abstract

Recently an exciting new mechanism of hydrosilylation had been found in experiments with the ruthenium–silylene complex $[Cp^*(i\text{-}Pr_3P)Ru(H)_2Si(H)Ph \cdot OEt_2][B(C_6F_5)_4]$ by Glaser and Tilley. The mechanism of the hydrosilylation and possible alternative pathways are investigated with quantum chemical methods utilizing the B3LYP method, a double zeta pseudopotential basis set for iron and ruthenium and the 6-31G* basis set for all other elements. Starting from the model complex $[Cp(H_3P)Ru(H)_2Si(H)Ph]^+$ the coordination of ethene at the silicon atom leads preferably to the hydrosilylation of a terminal Si–H-bond. The analysis of the electron density distribution of the catalytic active complex shows surprising bond features between Ru and Si. The Ru–Si bond is bridged by two hydrogen atoms.

The [2 + 2]-cycloaddition of the alkene to the Ru–Si-bond, which would be a reasonable alternative reaction pathway, was not observed. It is necessary to make drastic changes in the ligand environment of the transition metal–silicone complex to observe cycloaddition reactions. With complexes of the type $(OC)_4M{=}Si(H)Ph$ (M = Ru, Fe) the cycloaddition could be a serious alternative to the hydrosilylation.

Keywords: Homogeneous catalysis; Hydrosilylation; Ruthenium; Iron; Si ligands; DFT calculations

1. Introduction

The hydrosilylation is an important reaction, which is used in organosilicon chemistry, in organic synthesis, in dendrimer and polymer synthesis [1,2]. Hydrosilylation is performed mainly with transition metal catalysts. The Chalk–Harrod-mechanism – or similar mechanisms – are mainly accepted for this type of catalytic reaction [3,4]. The coordination of the alkene at the transition metal, the oxidative addition of the Si–H-bond, the insertion of the coordinated alkene into the M–H-bond and at last the reductive elimination of the product are the main steps of this mechanism (see Scheme 1).

Transition metal silylene complexes are highly reactive compounds [5], which are postulated as – respectively proved to be – intermediates in a number of catalytic and stoichiometric reactions [6,7]. There is no accepted hydrosilylation mechanism with a transition metal silylene as intermediate [8]. Tilley and Glaser reported recently about a possible new mechanism of hydrosilylation, which probably proceeds via a direct insertion of the alkene into a Si–H-bond of a ruthenium–silylene complex [9]. The starting complex for this catalytic cycle is $[Cp^*(i\text{-}Pr_3P)Ru(H)_2Si(H)Ph \cdot Et_2O][B(C_6F_5)_4]$ ($Cp^* = \eta^5\text{-}C_5Me_5$). The coordinated diethylether molecule is easily cleaved off in solution, providing the cation $[Cp^*(i\text{-}Pr_3P)Ru(H)_2Si(H)Ph]^+$ as the presumed catalytic active complex. The authors tested this new catalyst with different alkenes and obtained alkylsilanes in 57–94% yield. The hydrosilylation of $PhSiH_3$ with an excess of C_2D_4 yields exclusively $Ph(H)_2Si{-}CD_2{-}CD_2{-}H$. Catalytic hydrosilylation reactions have previously been found to afford mixtures of isotopomers with deuterated substrates via reversible olefin oxidation steps. The importance of this new type of catalytic reaction and the possible implication for preparative purposes has been highlighted

* Tel.: +49 3731 392050; fax: +49 3731 394058.
E-mail address: uwe.boehme@chemie.tu-freiberg.de.

0022-328X/$ - see front matter © 2006 Elsevier B.V. All rights reserved.
doi:10.1016/j.jorganchem.2006.01.021

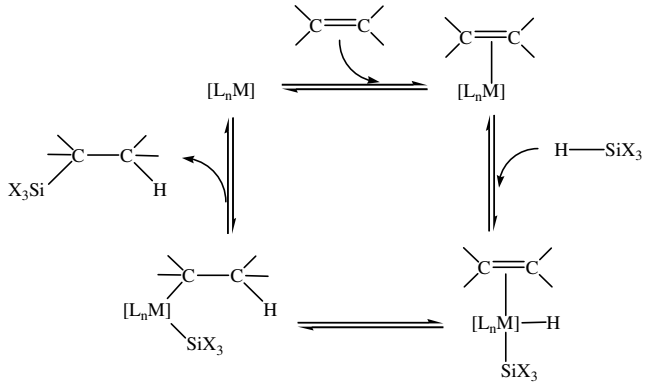

Scheme 1. Chalk–Harrod-mechanism of the hydrosilylation of olefines.

recently [8]. The intermediates proposed in Scheme 2 have not yet been proved experimentally. Other mechanisms would also be possible. A quantum chemical study which supports the mechanism in Scheme 2 has been published recently [10].

The quantum chemical study presented herein was performed in order to obtain a deeper insight into the mechanism of this new type of hydrosilylation and to understand why there was not observed any [2 + 2]-cycloaddition of the alkene to the Ru–Si-bond, which would be a reasonable alternative reaction pathway. The calculations have been performed with density functional theory [11,12]. The model compound $[Cp(H_3P)Ru(H)_2Si(H)Ph]^+$ was used in place of $[Cp^*(i\text{-}Pr_3P)Ru(H)_2Si(H)Ph]^+$, which was used for the experimental work. Ethene was used as model alkene. The stationary points were localized on the singulet potential energy surface and characterized as minima or transition states by calculating the Hessian-Matrices. Further characterization of the reaction profiles was achieved by following the intrinsic reaction coordinates (IRC) [13,14]. Mainly energy differences between the local minima and transition states on the potential energy surface are discussed throughout this paper. Only selected geometric parameters of the molecules under investigation will be discussed in order to keep this paper concise.

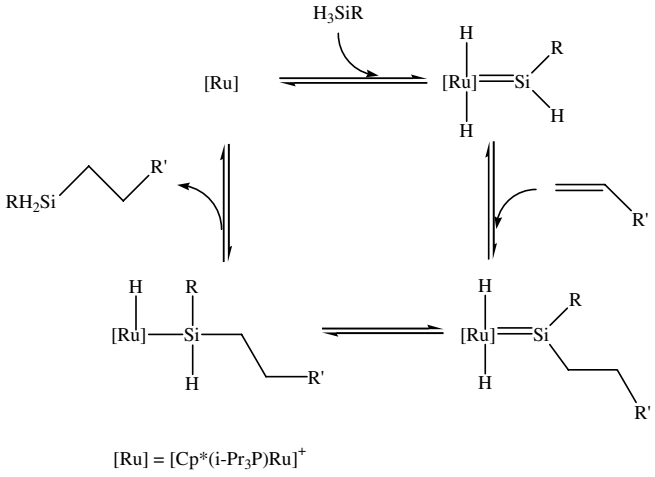

Scheme 2. Proposed hydrosilylation mechanism from Glaser and Tilley.

2. Results and discussion

2.1. Structure and properties of $[Cp(H_3P)Ru(H)_2Si(H)Ph]^+$ (2)

It was shown experimentally that the ether molecule in $[Cp^*(i\text{-}Pr_3P)Ru(H)_2Si(H)Ph \cdot Et_2O]^+$ is weakly bound to the silicon atom, since it is fast replaced by THF or Ph_2CO in CD_2Cl_2 solution [9]. The calculated free energy difference for the cleavage of the ether molecule from the model compound $[Cp(H_3P)Ru(H)_2Si(H)Ph \cdot Et_2O]^+$ (**1**) is 8.3 kJ mol^{-1} (see Scheme 3). The ruthenium cation $[Cp(H_3P)Ru(H)_2Si(H)Ph]^+$ (**2**), which is not stabilized by donor molecules, has surprising bond features along the Ru–Si-bond (Fig. 1). This bond axis is bridged by two hydrogen atoms. The topological analysis of the electron density distribution [15] of this cation shows, that there are bond critical points between Ru and Si, as well as between Ru–H and H–Si. The analysis of the molecule orbitals with the NBO-method [16] shows furthermore, that there are three centre bonds between Ru–H–Si. Such bridging Ru–H–Si-bonds have been proved to exist with X-ray structure analyses in other ruthenium complexes [17–23]. Non-classical interligand interactions are discussed also for hydrido-silyl-complexes of other transition metals, see for instance [24,25]. The presence of diethylether or other donor molecules in **1** has probably prevented the observation of such interactions until today.

Further investigation of the bonds between Ru–H and Si–H in this square arrangement of atoms was undertaken by relaxed scans of the potential energy surface (PES). Two different basis sets have been employed for this purpose. Basis set 1 (BS1) describes all main group elements with the 6-31G(d) basis set, as it was done with all other molecules in this paper. Basis set 2 (BS2) uses also 6-31G(d) for the main group elements plus an additional p-polarization function for the two bridging hydrogen atoms. This basis set contains provision for polarization of the s-orbitals at these two hydrogen atoms and gives them more flexibility in the bridged bonding mode [26]. The use of BS2 instead of BS1 changes the total energy of molecule **2** up to 9 kJ/mol during the PES scans (compare Fig. 3), but the overall geometrical features of the molecule are the same with both basis sets. The angle H–Ru–H was widened starting from the equilibrium geometry (see Fig. 2). This angle is rather flexible since the energy of the molecule increases only about 11–12 kJ/mol, when this angle is widened over 25°. There is a rehybridization of bonds in this complex when the two hydrogen atoms are no longer in a bridging situation but are exclusively bound to the ruthenium atom. The change in the bonding mode of the hydrogen atoms causes an inflexion point in the graph (angle H–Ru–H in Fig. 2). This hypothetical process takes place at 111° with BS1 and at 117° with the more flexible basis set BS2. The widening

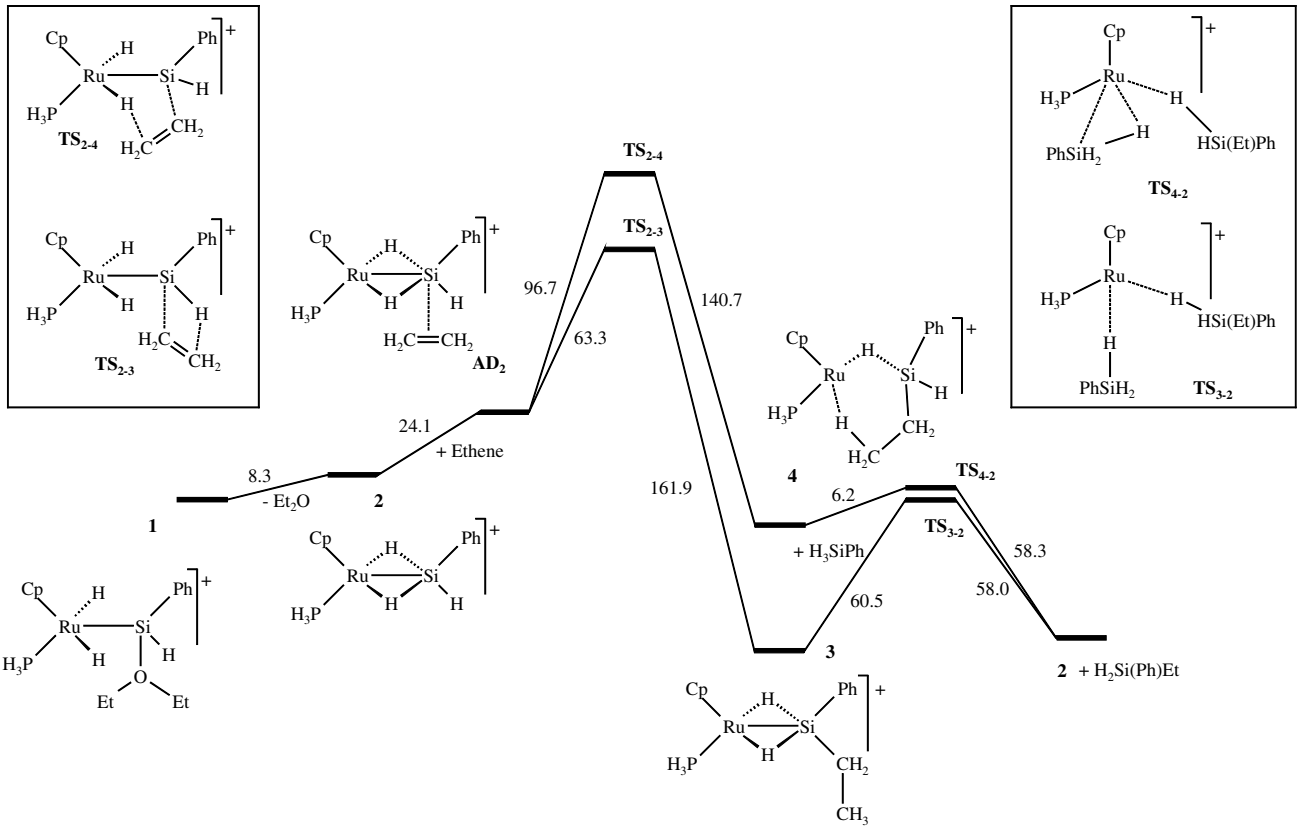

Scheme 3. Energy profile for the cleavage of diethylether from **1**, the coordination of ethene at the silicon atom and subsequent insertion steps into the Si–H-bonds (Gibb's free energy in kJ mol^{-1}).

of the angle H–Si–H leads to a much bigger rise in total energy (17–20 kJ/mol higher energy for 13° widening). These PES scans demonstrate that the ruthenium atom has much more flexibility and spatial more extended orbitals than the silicon atom to adopt to a change in the ligand environment.

The arbitrary elongation of the Ru–Si-bond starting from the equilibrium geometry of **2** yields further insight into the bond properties between Ru and Si. The distortion of the molecule geometry can be described with the schematic representation in Fig. 3. The elongation of the Ru–Si distance to more than 2.4 Å gives rise to a rapid increase of the total energy of the molecular system. At 2.8 Å the Ru–H bonds are broken and only weak interactions between Ru and Si are left. Beginning at 3.0 Å the SiH_3-group rotates around the phenyl-Si axis. This brings one of the hydrogen atoms in a suitable position to form a hydrogen bridge to the ruthenium atom and allows minimal stabilization of the system. This hypothetical process is reflected by an inflexion point in the graph with B3LYP/BS1. With B3LYP/BS2 the same process proceeds without an inflexion point in the graph. The energy necessary to decompose **2** into the fragments $[CpRu(PH_3)]^+$ and H_3SiPh is 82.6 kJ/mol (with B3LYP/BS1). Of course the highly reactive $[CpRu(PH_3)]^+$ would be stabilized in solution by other potential reaction partners or donor molecules. But this calculated process gives us further evidence that the bridging hydrogen atoms are not mainly bound to the ruthenium atom, but at least bound to the silicon atom with the same strength.

How compound **2** does react with alkenes? Different possible coordination modes of ethene at this cation have been investigated in order to answer this question. These are: (a) cycloaddition at the Ru–Si-bond, (b) coordination at the silicon atom, (c) coordination at the ruthenium atom. All efforts failed to find the hypothetic product of the cycloaddition of **2** with ethene via geometry optimization (path a). These optimizations gave structures which could be classified as local minima in the reaction pathways b or c. Obviously the Ru–Si-bond in **2** is shielded by surrounding ligands and substituents in that way, that the formation of a ruthenium–silacyclobutane becomes impossible.

2.2. Mechanism of hydrosilylation

The coordination of the ethene molecule at the silicon atom (path b) leads primary to the formation of the adduct $\mathbf{AD_2}$. The distance from the silicon atom to the carbon atoms of ethene is 3.6 Å. The bridging Si–H-bond opposite to the ethene molecule is slightly elongated (1.732 Å in $\mathbf{AD_2}$, 1.708 Å in **2**). All other geometrical parameters of the $[Cp(H_3P)Ru(H)_2Si(H)Ph]$-unit are very similar to **2**. The small changes of the geometry of the Ru–Si-cation and the long distance between ethene and the silicon atom

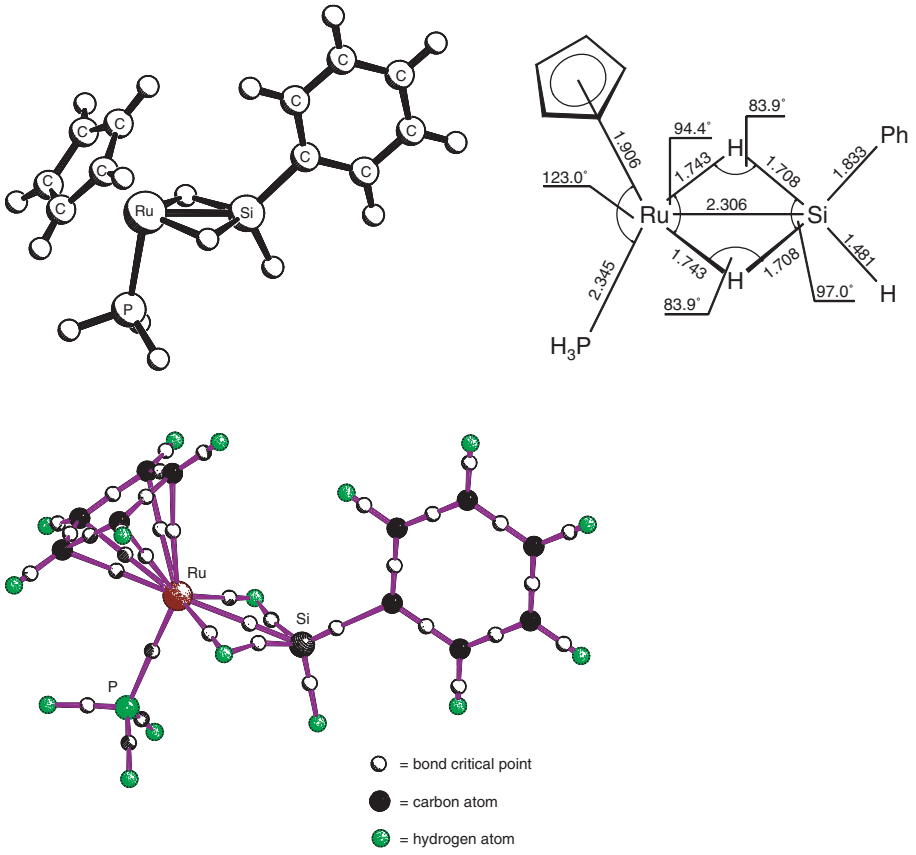

Fig. 1. Optimized geometry (top, bond lengths in Å, angles in °) and representation of bond critical points (bottom) of $[Cp(H_3P)Ru(H)_2Si(H)Ph]^+$ (**2**).

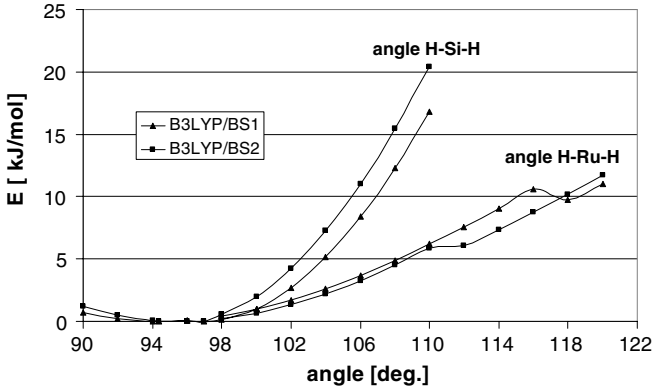

Fig. 2. Energy profiles of relaxed potential energy surface scans (PES) starting from **2**.

explain the small energy necessary to form the adduct (24.1 kJ/mol). This adduct allows access to two possible reaction pathways: the insertion of the ethene molecule into the terminal Si–H-bond or the insertion into one of the bridging Si–H-bonds. It was possible to localize transition states and reaction products for both reaction pathways. An activation energy of 63.3 kJ mol^{-1} is necessary to reach the transition state $\mathbf{TS_{2-3}}$ from $\mathbf{AD_2}$. The geometry of this transition state is shown in Fig. 4. The distance Ru–Si is elongated to 2.348 Å in $\mathbf{TS_{2-3}}$ compared to the same bond in **2** with 2.306 Å. The hydrogen atoms are no longer in a bridging position between Ru and Si; they are exclusively bound to the ruthenium atom. The terminal Si–H-bond is elongated to 1.565 Å, the C–C-double bond of the ethene molecule is gradually elongated and the carbon atoms of ethene are slightly pyramidalized. The distance between Si and C2 is 2.030 Å and the carbon atom C1 is with 1.734 Å still rather far away from the terminal hydrogen atom. Therefore we can designate $\mathbf{TS_{2-3}}$ in accordance with the Hammond postulate as an early transition state.

The mechanism described here is very similar to that proposed in [10]. The formation of the adduct $\mathbf{AD_2}$ from **2** requires 24.1 kJ/mol (15.9 kJ/mol in [10]), from $\mathbf{AD_2}$ to $\mathbf{TS_{2-3}}$ 63.3 kJ/mol (41.9 kJ/mol), and from $\mathbf{TS_{2-3}}$ to **3** −161.9 kJ/mol (−148.2 kJ/mol). There have been described three stationary points around $\mathbf{AD_2}$ in the calculated mechanism of Beddie and Hall [10]. This might be possible due to the presence of a flat potential energy surface around this ethylene complex.

The other possible reaction pathway is the insertion of ethene into the bridging Si–H bond. The activation barrier to reach the transition state $\mathbf{TS_{2-4}}$ for this insertion is 96.7 kJ mol^{-1}. Similar as in $\mathbf{TS_{2-3}}$ the hydrogen atoms in $\mathbf{TS_{2-4}}$ are bound only to the ruthenium atom (Fig. 4). The distance between the silicon atom and C2 is 2.054 Å, the distance between C1 and the reacting hydrogen atom is 1.701 Å. Due to these rather long distances one should designate $\mathbf{TS_{2-4}}$ also as an early transition state. The

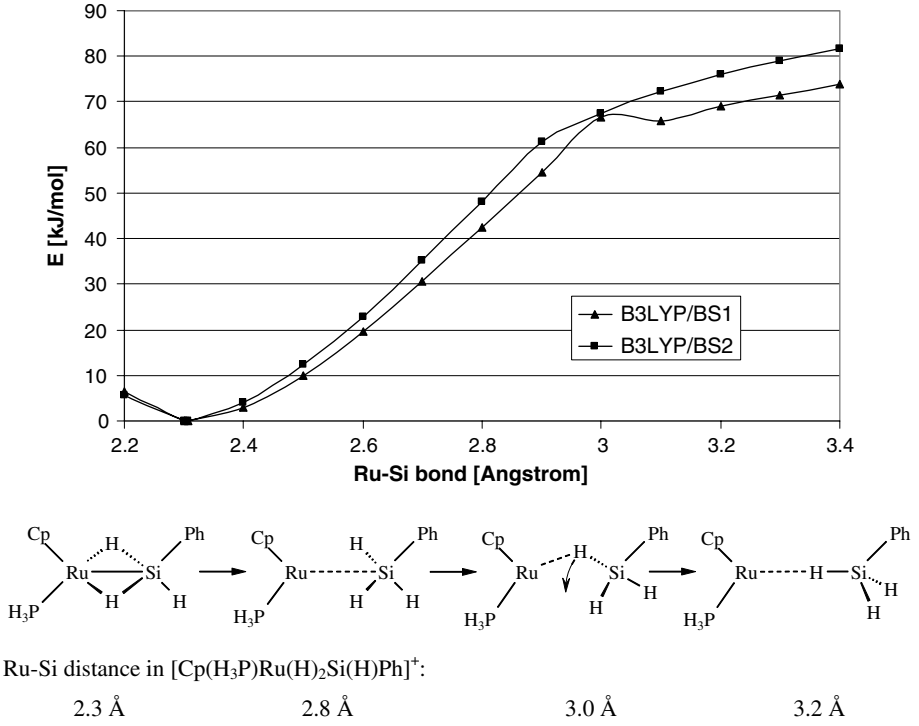

Fig. 3. Energy profiles for the elongation of the Ru–Si-bond of **2** from relaxed PES scan (top), and schematic representation of the molecule distortion (bottom).

further reaction from **3** or **4** to the product of hydrosilylation $H_2Si(Ph)Et$ was calculated with another substrate molecule H_3SiPh. The transition states $\mathbf{TS_{4-2}}$ and $\mathbf{TS_{3-2}}$ are accessible via rather small activation energies of 6.2 and 60.5 kJ mol^{-1}, respectively.

The coordination of ethene at the ruthenium atom of **2** would open another possible reaction pathway. This coordination leads to a substantial change of the coordination environment at the ruthenium atom. The transition state $\mathbf{TS_{2-5}}$ is reached with an activation energy of 85.2 kJ mol^{-1}. One of the ruthenium–hydrogen bonds is broken in the transition state (Fig. 5). The distance Ru–Si is clearly longer than in **2** (2.720 Å). The ethene molecule is still far away from the ruthenium atom (Ru···C1 = 3.522 and Ru···C2 = 3.474 Å). The cyclopentadienyl ligand, the phosphane, ethene and H_3SiPh are coordinated at the ruthenium atom in **5** (Fig. 5). Phenylsilane is bound via one hydrogen atom at the ruthenium atom. The distance Ru–Si is 2.995 Å and the AIM analysis shows that there is no bond critical point between the ruthenium and the silicon atom. The cation **5** is a minimum on the potential energy surface. The insertion of the ethene molecule into the Ru–H-bond gives the complex **6** which has an η^2-coordinated ethyl group and an η^1-coordinated SiH_2Ph. The reaction of **6** with one molecule H_3SiPh has an activation barrier of 94.9 kJ mol^{-1} to the transition state $\mathbf{TS_{6-2}}$. (Please notice that $\mathbf{TS_{6-2}}$ is not a true transition state since it has two imaginary frequencies. This puts the last step into question.) The ruthenium atom gains a lot of coordinative flexibility if the double hydrogen bridged silane ligand is moved out of the η^3-bonded mode. One possible rearrangement of ligands around the ruthenium atom is described in Scheme 4. Other subsequent rearrangements are imaginable. Two further pathways have been described in [10] and were assigned there as Chalk–Harrod and modified Chalk–Harrod mechanisms.

To compare both mechanisms from Schemes 3 and 4 one can say that on one hand we have the coordination of the alkene at the ruthenium atom which has a reasonable activation energy (Scheme 4). But the further reaction from the molecules **5** and **6** to the product of hydrosilylation has a second activation barrier via $\mathbf{TS_{6-2}}$ of 94.9 kJ mol^{-1}. The presence of two such activation barriers makes this reaction pathway rather improbable. On the other hand there is a similar activation energy when we assume a coordination of the alkene at the silicon atom. This pathway leads via η^3-coordinated silane complex **3** to the product of hydrosilylation and regenerates the key complex **2**. This pathway (Scheme 3) seems to be the favourable one. Since we have a reasonable activation energy in the first step via $\mathbf{AD_2}$ and $\mathbf{TS_{2-3}}$, leading to an low energy intermediate (**3**). From there it is only a small step to the final product of the catalytic cycle. The activation energy (ΔG) for the non catalyzed hydrosilylation of ethene with H_3SiPh is 304 kJ mol^{-1}. The activation energies necessary to perform the hydrosilylation with the catalyst–substrate complex **2** are much smaller. The highest barrier from **2** via $\mathbf{AD_2}$, $\mathbf{TS_{2-3}}$ to **3** has an activation energy of 87.4 kJ mol^{-1}. The results of the quantum chemical calculations up to this point are summarized in Scheme 5. The

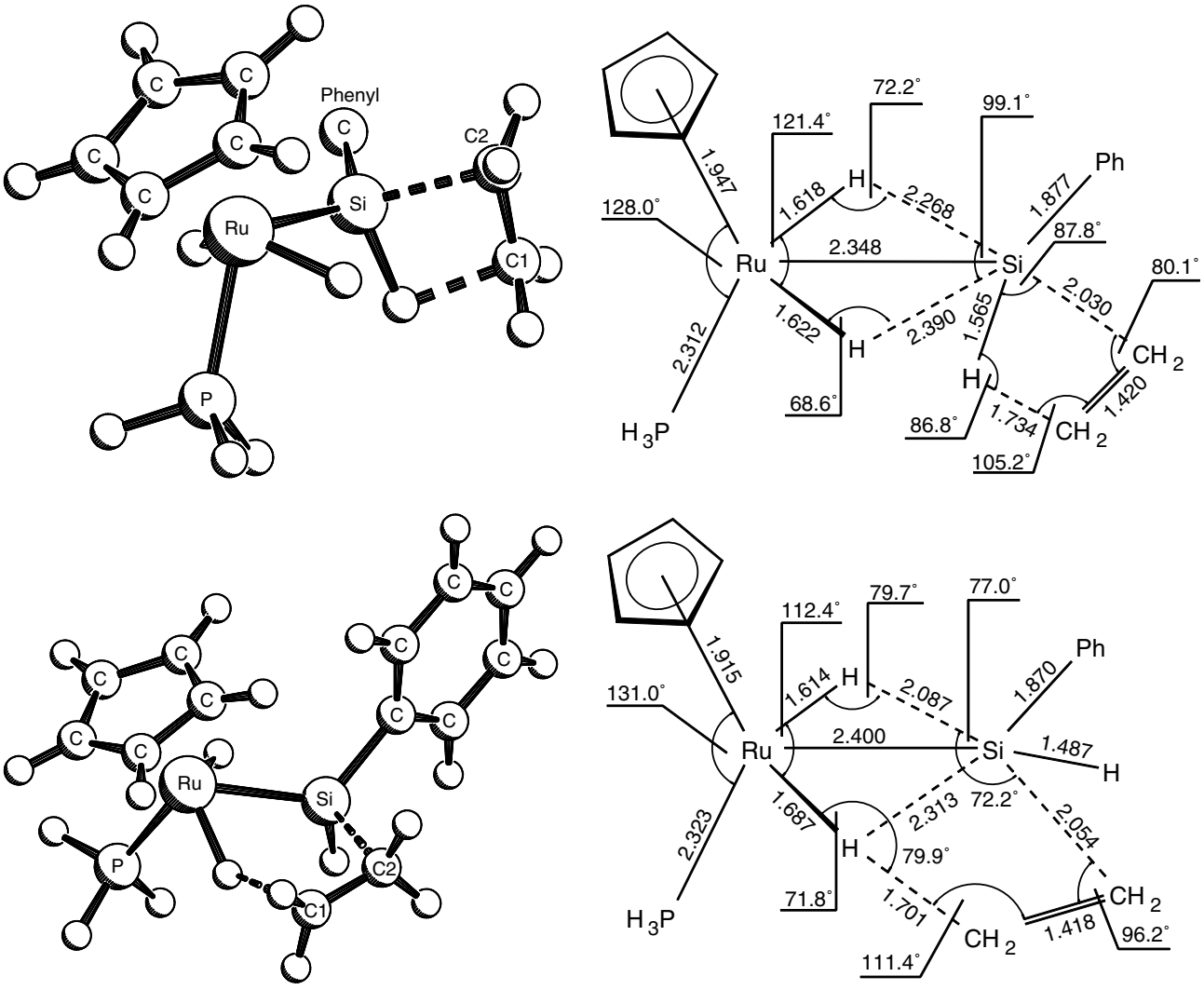

Fig. 4. Optimized geometry of the $\mathbf{TS_{2-3}}$ (top, atoms of the phenyl ring are omitted for claritiy) and $\mathbf{TS_{2-4}}$ (bottom; bond lengths in Å, angles in °).

key intermediate of the catalytic hydrosilylation is the η^3-bound silane complex. The coordination of alkene and the insertion into the terminal Si–H-bond are fundamental steps of this catalytic process.

2.3. [2 + 2]-Cycloaddition vs. hydrosilylation

As already mentioned in Section 2.1 the double hydrogen bridged ruthenium–silane complex **2** is not accessible to a cycloaddition reaction. That arises the question what happens if we remove the bridging hydrogen atoms in the complex **2**? Formally this could be described with the Eq. (1). The free energy (ΔG) which is necessary to obtain **7** from **2** is 77.1 kJ mol^{-1}. Practical similar compounds have already been synthesized. For instance the Ru–silylene complex **9** in Eq. (2) was synthesized by treating the silyltriflate **8** with 1 equiv. of $Li(Et_2O)_2B(C_6F_5)_4$ in CH_2Cl_2 [27]. Translated into the world of our model complexes this would mean that we take complex **10**, which has the same basic structural features like the experimental prepared complex **9**. Now one of the phosphane ligands is to be removed (Eq. (3)). This reaction requires 103.5 kJ mol^{-1} of free energy.

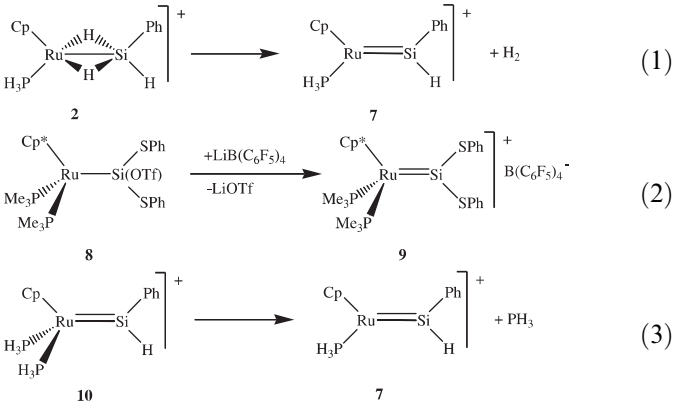

Removal of the two bridging hydrogen atoms from **2** gives the silylene complex **7**. The reactivity of this complex with ethene was also investigated with quantum chemical methods. One possible reaction is the direct insertion of the

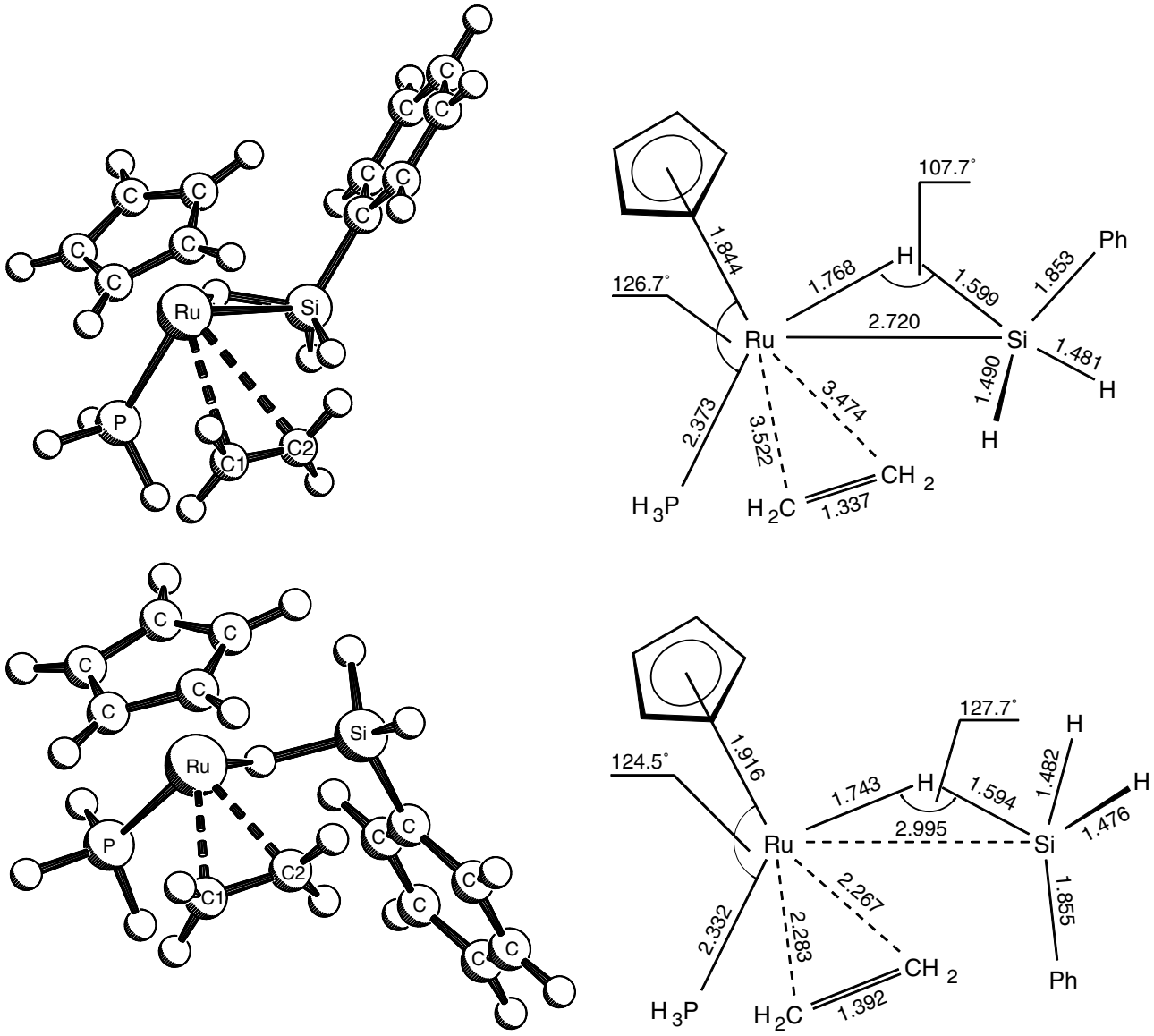

Fig. 5. Optimized geometry of $\mathbf{TS_{2-5}}$ (top) and **5** (bottom; bond lengths in Å, angles in °).

alkene into the Si–hydrogen bond. This reaction requires 49.7 kJ mol^{-1} activation energy. Far less activation energy leads to a product which has one ethene molecule coordinated at the Ru atom (**12**). The bonding properties of this reaction product are not quite clear. An analysis of bond critical points was performed. This reveals that there are only bonds between the Ru-atom and the alkene. There is no bond critical point between the alkene and the silicon atom. That means **12** is no cycloaddition product but should be rather considered as ruthenium complex with ethene as neutral donor ligand (see Scheme 6).

The ruthenium complex **10** with two phosphane ligands at the ruthenium atom has a different reactivity compared to **7** (see Scheme 7). The bonding in cationic ruthenium silylenes of this type has been investigated in detail by Arnold with DFT calculations [28]. The free energy to reach the transition state $\mathbf{TS_{10-13}}$ is 77.2 kJ mol^{-1}. It was also possible to find a cycloaddition product (**14**) and to localize the transition state $\mathbf{TS_{10-14}}$ which connects **10** with **14**. The activation energy for that reaction is 102.7 kJ mol^{-1}. The product of this cycloaddition reaction is the highest local minimum on the potential energy surface in Scheme 7. In all probability the reverse reaction from **14** to **10** will occur, since the activation energy from **10** to $\mathbf{TS_{10-14}}$ is only 27.5 kJ mol^{-1}. This high energy character of **14** will prevent the experimental access to this cycloaddition product. The hydrosilylation starting from **10** should be possible, but this compound has a reduced reactivity compared to **7** due to the presence of the second phosphane ligand.

The Ru–Si-complexes **2**, **7**, and **10** bearing around the ruthenium atom a cyclopentadienyl and one or two phosphine ligand are not accessible to cycloaddition reactions. There must be made rigorous changes in the ligand environment around the ruthenium atom in order to facilitate cycloaddition. There are known some base stabilized metal–silylene complexes which bear only carbonyl ligands

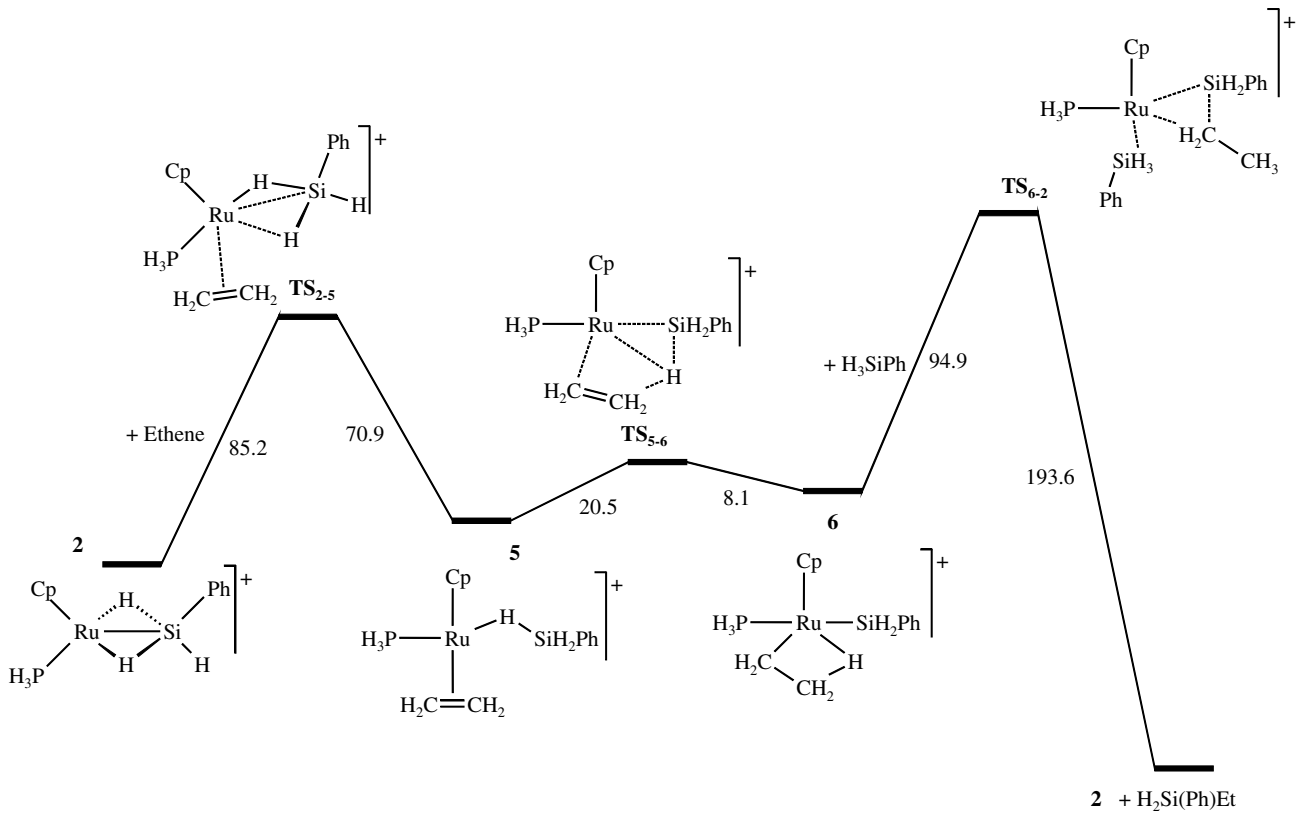

Scheme 4. Energy profile for the coordination of ethene at the ruthenium atom and subsequent insertion (Gibb's free energy in kJ mol^{-1}).

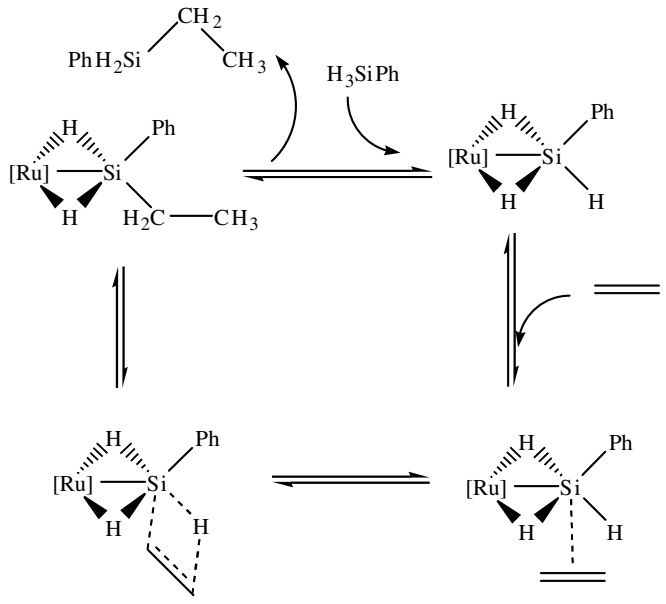

Scheme 5. Calculated mechanism of hydrosilylation.

around the transition metal atom (Fig. 6). These complexes have been synthesized by Zybill and coworkers [29–32]. The iron complex is the one which is best investigated. It is possible to remove the stabilizing hexamethylphosphoric acid triamide (HMPA) by heating the complex.

What is the reactivity of such transition metal silylene complexes? According to the calculated energy profiles in Scheme 8 it should be possible to observe hydrosilylation and cycloaddition with the ruthenium and the iron complex. The hydrosilylation reaction requires activation energy of 81.2 for the ruthenium and 83.7 kJ mol^{-1} for the iron complex. The cycloaddition reaction requires activation energy of 79.1 for the ruthenium and 86.2 kJ mol^{-1} for the iron complex. The activation energies for both reactions are very similar. The hydrosilylation product is thermodynamic more stabile. The tetracarbonyl-metal fragment provides a flexible ligand framework which is able to adopt to different substituents and which provides suitable orbitals for a cycloaddition reaction [33].

3. Summary

The quantum chemical investigation of the possible reaction pathways starting from the cation **2** and ethene shows, that (a) a classical [2 + 2]-cycloaddition at the Ru–Si-bond can be excluded; (b) the coordination of ethene at the silicon atom leads preferably to the hydrosilylation of a terminal Si–H-bond; and (c) the coordination of ethene at the ruthenium atom leads to a ruthenium–ethene complex.

The favoured reaction pathway on the singulet potential energy surface is the reaction from **1** via **2** to **3**. This is due to the low activation barrier and the highly exothermic reaction. The quantum chemical calculations presented herein do confirm the hydrosilylation mechanism which was proposed by Glaser and Tilley on the basis of experimental work. The catalytic active complex

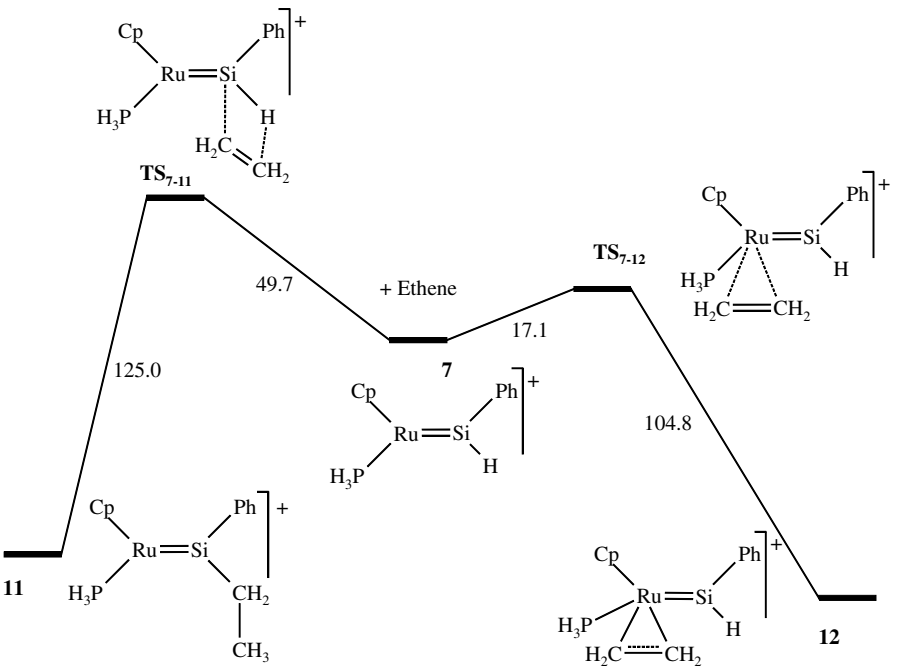

Scheme 6. Energy profile for the reaction of **7** with ethene (Gibb's free energy in kJ mol^{-1}).

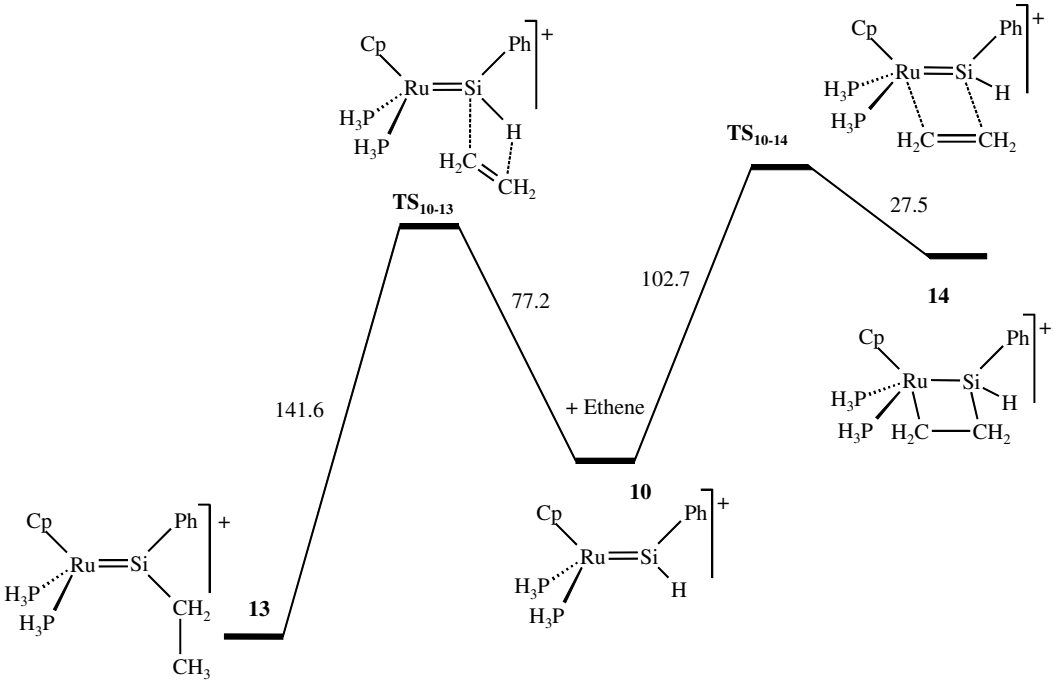

Scheme 7. Energy profile for the reaction of **10** with ethene (Gibb's free energy in kJ mol^{-1}).

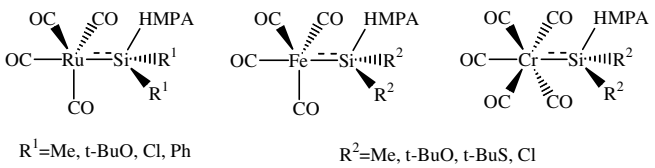

Fig. 6. Examples for base stabilized transition metal silylene complexes (HMPA, hexamethylphosphoric acid triamide).

has a nonclassical η^3-bonded silane ligand. This unusual dihydrogen bridged geometry is necessary to ease the insertion of the alkene into the terminal Si–H-bond. The ruthenium atom in **2** is able to bind these hydrogen atoms if necessary, compare transition state $\mathbf{TS_{2-3}}$. On the other hand this molecular system has enough flexibility to release the product of the hydrosilylation – including those two hydrogen atoms – in presence of other potential reaction partners. The unexpected hydrogen bridged

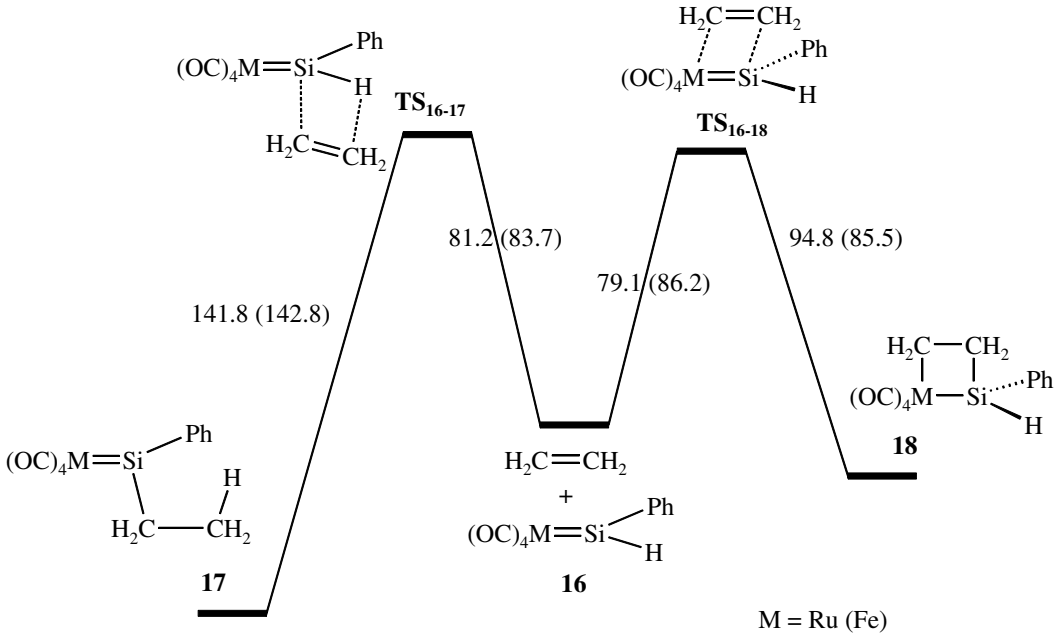

Scheme 8. Energy profile for the reaction of **16** with ethene (Gibb's free energy in kJ mol^{-1}, values in parenthesis are for the iron compounds).

structure of the ruthenium–silylene complex **2** deserves further experimental investigation. It would be a challenging task for the future to construct more ruthenium complexes with nonclassical bonded substrates which could perform other catalytic reactions.

A cycloaddition reaction might only occur with transition metal carbonyl silylene complexes $(OC)_nM{=}SiR_2$ (R = H, alkyl, aryl). But even then the cycloaddition has to compete with the hydrosilylation if there are hydrogen atoms at the silicon atom! The situation is changed completely for heteroatom substituted silylene complexes. Such silylene complexes might undergo in the presence of alkenes cycloaddition, dimerize, or act as silylene transfer reagents under formation of silacycles or polymerization of the silylene [31,33–35].

4. Computational details

The DFT calculations have been performed with the programme suite GAUSSIAN 03 [36]. All molecular geometries have been fully optimized. Beckes three parameter hybrid exchange functional in combination with the correlation functionals of Lee, Yang and Parr (B3LYP) was the used DFT method [11,12]. Geometry optimizations and frequency calculations have been performed with an effective core potential and a valence double zeta basis set for ruthenium and iron [LANL2DZ, 37] and the basis set 6-31G(d) for all main group elements [38,39]. An additional polarization function of f-type has been used for the elements ruthenium and iron [40]. This basis set is denoted as BS1.

All optimized geometries were characterized as minima with 0 or as transition states with one imaginary frequency by calculating the Hessian matrices. $\mathbf{TS_{6-2}}$ (Scheme 4) has two imaginary frequencies. Up to now it was not possible to localize a true transition state in that case. The reaction pathways for all other transition states have been investigated more closely by following the intrinsic reaction coordinate (IRC) starting from the transition states [13,14].

Additional polarization functions of p-type have been employed for the bridging hydrogen atoms in **2** for the PES calculations in Section 2.1. This basis set is denoted as BS2 (LANL2DZ plus f-polarization function for the Ru-atom, 6-31G(d) for all main group elements, 6-31G(d,p) [38] for the two bridging H-atoms).

The energy values in the energy profiles are the Gibb's free energy of the molecules in kJ mol^{-1}. The analysis of the electron density distribution [15] and the NBO-analysis [16] have been performed with the programme codes implemented in GAUSSIAN 03.

Acknowledgements

I thank the Freistaat Sachsen for financial support and the computing centre of the TU Bergakademie Freiberg for computing time and support during installation of programmes.

References

[1] B. Marciniec (Hrsg.), Comprehensive Handbook on Hydrosilylation, Pergamon Press, Oxford, 1992.
[2] I. Ojima, The hydrosilylation reaction, in: S. Patai, Z. Rappoport (Eds.), The Chemistry of Organic Silicon Compounds, Wiley, Chichester, 1989, p. 1479.
[3] A.J. Chalk, J.F. Harrod, J. Am. Chem. Soc. 87 (1965) 16.
[4] S.B. Duckett, R.H. Perutz, Organometallics 11 (1992) 90.
[5] T.D. Tilley, Transition metals in organosilicon chemistry, in: N. Auner, J. Weis (Eds.), Organosilicon Chemistry VI, Wiley–VCH, Weinheim, 2005, p. 382.

[6] T.D. Tilley, Transition-metal silyl derivatives, in: S. Patai, Z. Rappoport (Eds.), The Chemistry of Organic Silicon Compounds, Wiley, Chichester, 1989, p. 1415.
[7] C. Zybill, Top. Curr. Chem. 160 (1991) 1.
[8] H. Brunner, Angew. Chem. 116 (2004) 2805;
H. Brunner, Angew. Chem., Int. Ed. Engl. 43 (2004) 2749.
[9] P.B. Glaser, T.D. Tilley, J. Am. Chem. Soc. 125 (2003) 13640.
[10] C. Beddie, M.B. Hall, J. Am. Chem. Soc. 126 (2004) 13564.
[11] A.D. Becke, J. Chem. Phys. 98 (1993) 5648.
[12] C. Lee, W. Yang, R.G. Parr, Phys. Rev. B37 (1988) 785.
[13] K. Fukui, Acc. Chem. Res. 14 (1981) 363.
[14] C. Gonzalez, H.B. Schlegel, J. Chem. Phys. 95 (1991) 5853.
[15] R.F.W. Bader, Atoms in Molecules. A Quantum Theory, Oxford University Press, Oxford, 1990.
[16] A.E. Reed, L.A. Curtiss, F. Weinhold, Chem. Rev. 88 (1988) 899.
[17] I. Atheaux, B. Donnadieu, V. Rodriguez, S. Sabo-Etienne, B. Chaudret, K. Hussein, J.-C. Barthelat, J. Am. Chem. Soc. 122 (2000) 5664.
[18] T. Ayed, J.-C. Barthelat, B. Tangour, C. Pradère, B. Donnadieu, M. Grellier, S. Sabo-Etienne, Organometallics 24 (2005) 3824.
[19] R. Ben Said, K. Hussein, J.-C. Barthelat, I. Atheaux, S. Sabo-Etienne, M. Grellier, B. Donnadieu, B. Chaudret, Dalton Trans. (2003) 4139.
[20] S.T.N. Freeman, F.R. Lemke, L. Brammer, Organometallics 21 (2002) 2030.
[21] N.M. Yardy, F.R. Lemke, L. Brammer, Organometallics 20 (2001) 5670.
[22] A.L. Osipov, S.F. Vyboishchikov, K.Y. Dorogov, L.G. Kuzmina, J.A.K. Howard, D.A. Lemenovskii, G.I. Nikonov, Chem. Commun. (2005) 3349.
[23] A.L. Osipov, S.M. Gerdov, L.G. Kuzmina, J.A.K. Howard, G.I. Nikonov, Organometallics 24 (2005) 587.
[24] G. Nikonov, J. Organomet. Chem. 635 (2001) 24.
[25] G. Nikonov, Angew. Chem. 113 (2001) 3457;
G. Nikonov, Angew. Chem., Int. Ed. Engl. 40 (2001) 3353.
[26] W.J. Hehre, L. Radom, P.v.R. Schleyer, J.A. Pople, Ab Initio Molecular Orbital Theory, Wiley, New York, 1986, p. 82.
[27] S.R. Klei, D. Tilley, R.G. Bergman, Organometallics 21 (2002) 4648.
[28] F.P. Arnold Jr., Organometallics 18 (1999) 4800.
[29] C. Zybill, G. Müller, Angew. Chem. 99 (1987) 683;
C. Zybill, G. Müller, Angew. Chem., Int. Ed. Engl. 26 (1987) 669.
[30] C. Zybill, G. Müller, Organometallics 7 (1988) 1368.
[31] C. Leis, D.L. Wilkinson, H. Handwerker, C. Zybill, G. Müller, Organometallics 11 (1992) 514.
[32] H. Handwerker, C. Leis, S. Gamper, C. Zybill, Inorg. Chim. Acta 198 (1992) 763.
[33] U. Böhme, [2 + 2]-cycloadditions of $(OC)_4Fe{=}SiMe_2$ – a theoretical study, in: N. Auner, J. Weis (Eds.), Organosilicon Chemistry VI, Wiley–VCH, Weinheim, 2005, p. 438.
[34] C. Leis, C. Zybill, Polyhedron 10 (1991) 1163.
[35] C. Zybill, D.L. Wilkinson, C. Leis, G. Müller, Angew. Chem. 101 (1989) 206;
C. Zybill, D.L. Wilkinson, C. Leis, G. Müller, Angew. Chem., Int. Ed. Engl. 28 (1989) 203.
[36] M.J. Frisch, G.W. Trucks, H.B. Schlegel, G.E. Scuseria, M.A. Robb, J.R. Cheeseman, J.A. Montgomery Jr., T. Vreven, K.N. Kudin, J.C. Burant, J.M. Millam, S.S. Iyengar, J. Tomasi, V. Barone, B. Mennucci, M. Cossi, G. Scalmani, N. Rega, G.A. Petersson, H. Nakatsuji, M. Hada, M. Ehara, K. Toyota, R. Fukuda, J. Hasegawa, M. Ishida, T. Nakajima, Y. Honda, O. Kitao, H. Nakai, M. Klene, X. Li, J.E. Knox, H.P. Hratchian, J.B. Cross, C. Adamo, J. Jaramillo, R. Gomperts, R.E. Stratmann, O. Yazyev, A.J. Austin, R. Cammi, C. Pomelli, J.W. Ochterski, P.Y. Ayala, K. Morokuma, G.A. Voth, P. Salvador, J.J. Dannenberg, V.G. Zakrzewski, S. Dapprich, A.D. Daniels, M.C. Strain, O. Farkas, D.K. Malick, A.D. Rabuck, K. Raghavachari, J.B. Foresman, J.V. Ortiz, Q. Cui, A.G. Baboul, S. Clifford, J. Cioslowski, B.B. Stefanov, G. Liu, A. Liashenko, P. Piskorz, I. Komaromi, R.L. Martin, D.J. Fox, T. Keith, M.A. Al-Laham, C.Y. Peng, A. Nanayakkara, M. Challacombe, P.M.W. Gill, B. Johnson, W. Chen, M.W. Wong, C. Gonzalez, J.A. Pople, GAUSSIAN 03, Revision C.02, Gaussian, Inc., Wallingford, CT, 2004.
[37] P.J. Hay, W.R. Wadt, J. Chem. Phys. (1985) 299.
[38] P.C. Hariharan, J.A. Pople, Theor. Chim. Acta 28 (1973) 213.
[39] M.M. Francl, W.J. Pietro, W.J. Hehre, J.S. Binkley, M.S. Gordon, D.J. DeFrees, J.A. Pople, J. Chem. Phys. 77 (1982) 3654.
[40] A.W. Ehlers, M. Böhme, S. Dapprich, A. Gobbi, A. Höllwarth, V. Jonas, K.F. Köhler, R. Stegmann, A. Veldkamp, G. Frenking, Chem. Phys. Lett. 208 (1993) 111.